THE JOURNAL OF PHYSICAL CHEMISTRY A
A JOURNAL OF THE AMERICAN CHEMICAL SOCIETY

pubs.acs.org/JPCA Article

Probing the Effects of Size and Charge on the Monohydration and Dihydration of SiF_5^- and SiF_6^{2-} via Comparisons with BF_4^- and PF_6^-

Jacquelyn J. Mosely and Gregory S. Tschumper*

Cite This: *J. Phys. Chem. A* 2024, 128, 5637−5645 Read Online

ABSTRACT: This study systematically examines the interactions of the trigonal bipyramidal silicon pentafluoride and octahedral silicon hexafluoride anions with either one or two water molecules, ($SiF_5^-(H_2O)_n$ and $SiF_6^{2-}(H_2O)_n$, respectively, where n = 1, 2). Full geometry optimizations and subsequent harmonic vibrational frequency computations are performed using the CCSD(T) *ab initio* method with a triple-ζ correlation consistent basis set augmented with diffuse functions on all non-hydrogen atoms (cc-pVTZ for H and aug-cc-pVTZ for Si, O, and F; denoted as haTZ). Two monohydrate and six dihydrate minima have been identified for the $SiF_5^-(H_2O)_n$ systems, whereas one monohydrate and five dihydrate minima have been identified for the $SiF_6^{2-}(H_2O)_n$ systems. Both monohydrated anions have a minimum in which the water molecule adopts a symmetric double ionic hydrogen bond (DIHB) motif with C_{2v} symmetry. However, a second unique monohydrate minimum has been identified for SiF_5^- in which the water molecule adopts an asymmetric DIHB motif along the edge of the trigonal bipyramidal anion between one axial and one equatorial F atom. This C_s structure is more than 2 kcal mol^{-1} lower in energy than the C_{2v} local minimum at the CCSD(T)/haTZ level of theory. While the interactions between the solvent and ionic solute are quite strong for the monohydrated anions (electronic dissociation energies of ≈12 and ≈24 kcal mol^{-1} for the $SiF_5^-(H_2O)_1$ and $SiF_6^{2-}(H_2O)_1$ global minima, respectively), these values are nearly perfectly doubled for the dihydrates, with the lowest-energy $SiF_5^-(H_2O)_2$ and $SiF_6^{2-}(H_2O)_2$ minima exhibiting dissociation energies of ≈24 and ≈47 kcal mol^{-1}, respectively. Structures that form hydrogen bonds between the solvating water molecules also exhibit the largest shifts in the harmonic OH stretching frequencies for the waters of hydration. These shifts can exceed −100 cm^{-1} for the $SiF_5^-(H_2O)_2$ minimum and −300 cm^{-1} for the $SiF_6^{2-}(H_2O)_2$ minimum relative to an isolated H_2O molecule at the CCSD(T)/haTZ level of theory. This work also corrects the OH stretching frequency shifts for two dihydrate minima of PF_6^- that were previously erroneously reported (*J. Phys. Chem. A* **2020**, *124*, 8744−8752, DOI: 10.1021/acs.jpca.0c06466).

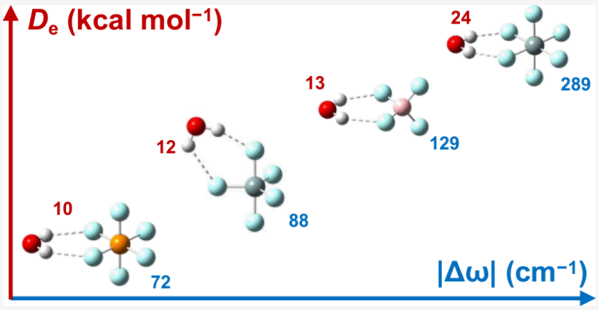

1. INTRODUCTION

The aqueous solvation of ions plays a crucial role in many fundamental biological, chemical, environmental, and industrial processes.[1−8] These include the regulation of many bodily functions,[1] stabilization and denaturization of biomacromolecules,[2−5] and the development of aqueous ion batteries.[6−8] Ion hydration is also of importance in the context of ionic liquids (ILs), since the presence of water, as an impurity or as a cosolvent, can alter the physicochemical properties of a given IL.[9−11]

The hydration of negatively charged ions is particularly interesting because a solvent water molecule has the potential to donate up to two hydrogen bonds to an anion. These ionic hydrogen bonds (IHBs) exist in two structurally and spectroscopically distinct motifs: the single IHB and double IHB (commonly abbreviated SIHB and DIHB, respectively). In SIHB structures, only one hydrogen atom from water interacts with the anion through a hydrogen bond while the other hydrogen remains free.[12] In contrast, both hydrogen atoms interact with the anion in the DIHB motif, usually in a symmetric manner.[13,14] SIHBs are commonly observed between water and atomic[15] or diatomic[16,17] anions, though some triatomic[14] species will also bind in this manner. DIHBs do not often occur between water and small atomic or diatomic anions; they are typically observed for larger anions with three or more atoms.[14,18] The DIHB hydration pattern can be seen for a series of fluorine-containing anions including the trigonal planar BeF_3^-,[19] the tetrahedral BF_4^-,[20,21] and the octahedral PF_6^-.[20,22] Considerable interest lies in characterizing these anions due to their nature as superhalogens, a class of molecules which exhibit electron affinity (EA) and vertical electron detachment energy (VDE) values larger than those of

Received: May 24, 2024
Revised: June 26, 2024
Accepted: June 27, 2024
Published: July 8, 2024

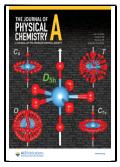

halogen atoms.[23,24] The large electron binding energies of these species frequently make them good candidates for components in ILs[25−27] and supersalts.[28−32]

The silicon pentafluoride anion, SiF_5^-, is another relevant superhalogen, though less commonly studied[23,24,33,34] relative to BF_4^- and PF_6^-.[11,26,27,35−43] These three anions have VDE values of or exceeding 9 eV,[34,35,38,44] and their neutral parent molecules have EA values around 6 eV.[23] The shared characteristics of BF_4^-, PF_6^-, and SiF_5^- provide an opportunity to probe the geometry dependence of microhydration patterns between the three singly charged anions. The trigonal bipyramidal geometry of SiF_5^- also bridges the gap in fundamental VSEPR geometries between tetrahedral BF_4^- and octahedral PF_6^-.

The closely related silicon hexafluoride dianion, SiF_6^{2-}, is also a molecule of interest as it has been shown to dissociate into SiF_5^- and F^-.[45,46] SiF_6^{2-} also shares an octahedral geometry with the isoelectronic PF_6^- ion, and both have histories of use in coordination chemistry.[47−49] The microscale hydration of the SiF_6^{2-} ion provides an opportunity to probe the charge dependence of microhydration patterns between the doubly charged SiF_6^{2-} ion and the singly charged SiF_5^- ion as well as the BF_4^- and PF_6^- ions, both of whose hydration patterns have been studied previously at both the microscale[20−22] and in the bulk phase.[37,40,50]

This study examines the effects of structure and charge on the microhydration of symmetric fluorinated anions by comparing the hydration patterns and energetics of the hydrated tetrahedral BF_4^- and octahedral PF_6^- anions with those for the hydrated trigonal bipyramidal SiF_5^- anion and the octahedral SiF_6^{2-} dianion. The microhydration of these systems will allow for an opportunity to better understand the fundamental water−water and water−anion interactions that occur in bulk hydrated systems[15,19,51−60] using a "ground-up" approach.[15] Previous work[21,22] detailed the importance of considering solvent−solvent interactions, as opposed to only solvent−solute interactions, when hydrating PF_6^- and BF_4^-. This work means to provide a similar analysis of configurations that are adopted when SiF_5^- and SiF_6^{2-} are each explicitly solvated with up to two water molecules, giving particular attention to dihydrates which can exhibit solvent−solvent interactions. A detailed analysis of the harmonic vibrational frequency shifts is also performed to complement what has been done in previous studies.[21,22,40] To the best of our knowledge, this study is the first which looks at the explicit hydration of SiF_5^- and SiF_6^{2-}.

2. COMPUTATIONAL DETAILS

The mono- and dihydrate structures of SiF_5^- and SiF_6^{2-} ($SiF_5^-(H_2O)_{1,2}$ and $SiF_6^{2-}(H_2O)_{1,2}$, respectively) reported in this study were fully optimized using second-order Møller−Plesset perturbation theory (MP2)[61] and the CCSD(T) coupled cluster method that includes all single and double substitutions along with a perturbative estimate of connected triple substitutions,[62−64] each in conjunction with Dunning's correlation consistent double- or triple-ζ basis set augmented with diffuse functions on all nonhydrogen (or "heavy") atoms (cc-pV*X*Z for H and aug-cc-pV*X*Z for Si, O, and F; denoted hereafter as ha*X*Z, where X = D, T).[65−67] Readers interested in the rationale for and naming schemes associated with these "heavy" augmented basis sets can find additional details in the Computational Details section of ref 21. Inspired by previously characterized $PF_6^-(H_2O)_{1,2}$ and $BF_4^-(H_2O)_{1,2}$ geometries,[21,22] the $SiF_5^-(H_2O)_{1,2}$ and $SiF_6^{2-}(H_2O)_{1,2}$ structures reported here were found by systematically distributing up to two water molecules around the faces and edges of the SiF_5^- trigonal bipyramid and SiF_6^{2-} octahedron.

Harmonic vibrational frequencies were computed analytically for each MP2 optimized structure to confirm each structure as a minimum on its respective potential energy surface. CCSD(T)/haTZ Hessians were obtained from the finite difference of analytic gradients after validating the accuracy of the procedure with the haDZ basis set for which the frequencies computed in this manner never differed by more than 0.1 cm^{-1} from those computed analytically. Additional optimizations and harmonic vibrational frequency computations were also performed on the isolated fragments of SiF_5^-, SiF_6^{2-}, and H_2O. The electronic dissociation energy of each complex was computed by taking the sum of the monomers' energies and subtracting the energy of the complex. With finite basis sets, this process introduces an inconsistency known as basis set superposition error (BSSE).[68,69] To evaluate the potential effects of BSSE on the computed dissociation energies, the Boys−Bernardi counterpoise procedure (CP)[70−72] was applied, following the protocol detailed elsewhere,[73] to the lowest-energy mono- and dihydrate minima for the $SiF_5^-(H_2O)_{1,2}$ and $SiF_6^{2-}(H_2O)_{1,2}$ systems. All MP2 calculations were performed with `Gaussian16`.[74] CCSD(T) optimizations were performed with the `Gaussian09`[75] optimizer using analytic gradients computed by `CFOUR`.[76] All CCSD(T) frequency computations were performed with `Molpro`.[77−79] The frozen-core approximation was employed in all MP2 and CCSD(T) computations, excluding from the correlation procedure the two core electrons for O and F atoms along with the ten core electrons for Si atoms. In all cases, pure angular momentum functions (5*d*, 7*f*, etc.) were used in place of their Cartesian counterparts.

3. RESULTS AND DISCUSSION

3.1. Structures and Energetics. When a water molecule interacts with either the SiF_5^- or SiF_6^{2-} ion, two structural motifs are observed for the mono- and dihydrate minima shown in Figures 1 and 2. The "DI_x" label indicates that x water molecules have formed double ionic hydrogen bonds (DIHBs) with a pair of fluorine atoms from the anion, an example of which can be seen in the C_s DI_1 monohydrate structure shown in the top left corner of Figure 1. When a second water molecule is added to the system, there is potential for hydrogen bonding to occur between the two water molecules. This arrangement is denoted by the "WI_y" label which indicates that y water molecules have formed a hydrogen bond with one fluorine atom from the anion and a hydrogen bond with another water molecule. An example of this type of motif can be seen the C_1 DI_1WI_1 dihydrate structure shown in the top right corner of Figure 1. For each motif, $x + y = n$ where n is the total number of water molecules in the system. The Cartesian coordinates and harmonic vibrational frequencies for the mono- and dihydrated SiF_5^- and SiF_6^{2-} complexes can be found in the Supporting Information.

3.1.1. $SiF_5^-(H_2O)_n$. The isolated SiF_5^- ion has a trigonal bipyramidal structure with D_{3h} symmetry. When the anion interacts with a single water molecule, its trigonal bipyramidal geometry gives rise to two distinct DIHB motifs producing OH···F contacts. One motif occurs in which the water molecule binds to symmetry equivalent F atoms along an

https://doi.org/10.1021/acs.jpca.4c03430
J. Phys. Chem. A 2024, 128, 5637−5645

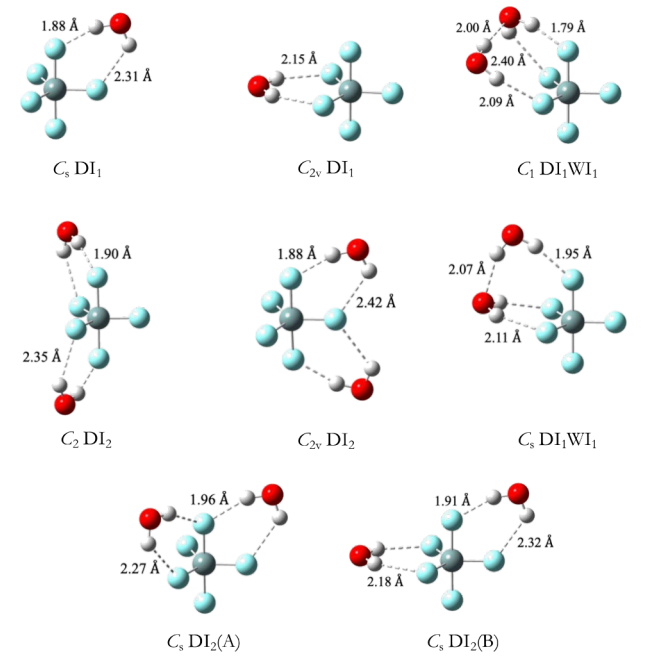

Figure 1. CCSD(T)/haTZ minima for the $SiF_5^-(H_2O)_n$ systems (where n = 1, 2), their corresponding point group symmetries, and unique OH···F and OH···O bond lengths (in Å).

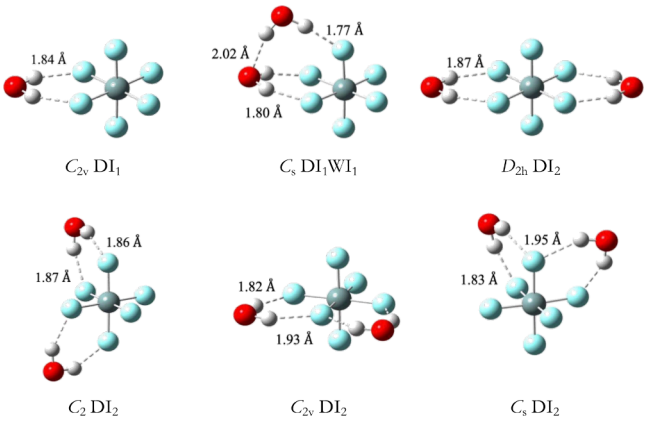

Figure 2. CCSD(T)/haTZ minima for the $SiF_6^{2-}(H_2O)_n$ systems (where n = 1, 2), their corresponding point group symmetries, and unique OH···F and OH···O bond lengths (in Å).

equatorial edge of the anion, resulting in two equivalent OH···F interactions and a complex with C_{2v} symmetry, as shown in the middle image in the top row of Figure 1, denoted C_{2v} DI$_1$. This symmetric DIHB motif is the structural counterpart for the monohydrates of both BF_4^- (C_{2v} DI$_1$ structure in Figure 1 of ref 21) and PF_6^- (C_{2v} Edge structure in Figure 1 of ref 22). In contrast, the second structural motif formed when SiF_5^- interacts with a water molecule is one in which one hydrogen from the water molecule binds to an equatorial fluorine atom of the anion while the other hydrogen binds to an axial fluorine atom, as shown in the top left corner of Figure 1, denoted C_s DI$_1$.

The CCSD(T)/haTZ optimized structure shows the axial Si−F distances are longer by about 0.05 Å in the isolated anion. Because the axial and equatorial F atoms in the SiF_5^- trigonal bipyramid are not symmetry equivalent, this second binding motif results in a C_s-symmetry complex with two nonequivalent OH···F contacts. The C_s DI$_1$ monohydrate global minimum consists of an asymmetric DIHB where, rather than having two identical 2.15 Å hydrogen bonds like the C_{2v} DI$_1$ local minimum, one OH···F bond in C_s DI$_1$ becomes slightly shorter at 1.88 Å while the other lengthens to 2.31 Å. The DIHB character of this asymmetric motif is still supported, however, by changes in the OH bond lengths (Supporting Information) and shifts in the harmonic vibrational OH stretching frequencies (Section 3.2). Although there is only a single minimum to consider for $BF_4^-(H_2O)_1$ and $PF_6^-(H_2O)_1$, the situation changes with these two minima identified for $SiF_5^-(H_2O)_1$. Interestingly, the CCSD(T)/haTZ electronic energy of the symmetric C_{2v} DI$_1$ structure is 2.12 kcal mol^{-1} higher than the C_s DI$_1$ minimum. The formation of a shorter H-bond to the axial position of SiF_5^- than the equatorial position (1.88 vs 2.31 Å) in the C_s global minimum monohydrate structure is consistent with the charge distribution on the F centers. A natural bond orbital (NBO) analysis has shown that there is a slightly greater concentration of negative charge on the axial F atoms.[46]

The dissociation energy (D_e) of the C_s DI$_1$ minimum is 12.21 kcal mol^{-1} when using CCSD(T) with the haTZ basis set, as shown in the top row of Table 1, which falls between the corresponding values for C_{2v} DI$_1$ monohydrates of BF_4^- and PF_6^- (13.17 and 10.67 kcal mol^{-1}, respectively). All the values in Table 1 are reported to two decimal places to facilitate comparison; the precision is not intended to reflect the

Table 1. CCSD(T)/haTZ Electronic Dissociation Energies (D_e in kcal mol^{-1}) of the BF_4^-, SiF_5^-, PF_6^-, and SiF_6^{2-} Monohydrate and Dihydrate Minima

$BF_4^-(H_2O)_n$		$SiF_5^-(H_2O)_n$		$PF_6^-(H_2O)_n$		$SiF_6^{2-}(H_2O)_n$	
Structure	D_e[a]	Structure	D_e	Structure	D_e[b]	Structure	D_e
			Monohydrates (n = 1)				
C_{2v} DI$_1$	13.17	C_s DI$_1$	12.21	C_{2v} DI$_1$[c]	10.67	C_{2v} DI$_1$	24.82
		C_{2v} DI$_1$	10.09				
			Dihydrates (n = 2)				
C_s DI$_1$WI$_1$	26.43	C_1 DI$_1$WI$_1$	24.13	C_s DI$_1$WI$_1$[d]	22.52	C_s DI$_1$WI$_1$	47.81
D_{2d} DI$_2$	25.12	C_2 DI$_2$	23.37	D_{2h} DI$_2$[e]	20.43	D_{2h} DI$_2$	47.76
C_s DI$_2$	24.73	C_{2v} DI$_2$	23.11	C_2 DI$_2$[e]	20.35	C_2 DI$_2$	47.70
		C_s DI$_1$WI$_1$	22.98	C_s DI$_2$[e]	20.10	C_{2v} DI$_2$	47.19
		C_s DI$_2$(A)	22.76			C_s DI$_2$	46.70
		C_s DI$_2$(B)	21.36				

[a]Ref 21. [b]Ref 22. [c]Labeled as "Edge" structure in ref 22. [d]Labeled as "WW-Edge-Face" structure in ref 22. [e]Labeled as "Edge−Edge" structure in ref 22.

https://doi.org/10.1021/acs.jpca.4c03430
J. Phys. Chem. A 2024, 128, 5637−5645

Table 2. Shifts in the CCSD(T)/haTZ Harmonic OH Stretching Frequencies ($\Delta\omega$ in cm^{-1}) Induced by Hydrogen Bonding in the BF_4^-, SiF_5^-, PF_6^-, and SiF_6^{2-} Monohydrate Global Minima Relative to the Symmetric a_1 and Antisymmetric b_2 OH Stretches for an Isolated Water Molecule (ω in cm^{-1}) along with the Irreducible Representations (irrep) Associated with Each Vibrational Mode

H_2O		$BF_4^-(H_2O)_1$		$SiF_5^-(H_2O)_1$		$PF_6^-(H_2O)_1$		$SiF_6^{2-}(H_2O)_1$	
irrep	ω	irrep	$\Delta\omega$[a]	irrep	$\Delta\omega$	irrep	$\Delta\omega$[b]	irrep	$\Delta\omega$
a_1	3814	a_1	−58	a′	−88	a_1	−17	a_1	−159
b_2	3924	b_2	−129	a′	−69	b_2	−72	b_2	−289

[a]Ref 21. [b]Ref 22.

accuracy of the computed energetics. To provide some context for these interactions, we note that all of the three monohydrate D_e values are at least twice as large as the D_e for the water dimer which is approximately 5 kcal mol^{-1} at similar levels of theory.[80,81] A comparison of the three monohydrate global minima reveals that D_e increases as the anions get smaller (PF_6^- < SiF_5^- < BF_4^-), which is consistent with the expectation that the negative charge is more localized in a smaller ion.

Six minima have been identified for the $SiF_5^-(H_2O)_2$ system by systematically distributing two water molecules around the faces and edges of the SiF_5^- trigonal bipyramid. These six SiF_5^- dihydrates are pictured in Figure 1 along with the two aforementioned monohydrate minima. For $SiF_5^-(H_2O)_2$, two DI_1WI_1 structures have been identified, with the C_1 isomer being the global minimum and the C_s local minimum lying about 1 kcal mol^{-1} higher at the CCSD(T)/haTZ level of theory. The global minima of the BF_4^- and PF_6^- dihydrates also exhibit the same solvent−solvent contacts. Similar to what was observed for the series of BF_4^-, SiF_5^-, and PF_6^- monohydrates, the D_e values of the dihydrate global minima increase as the anion becomes smaller. The first row of dihydrate data in Table 1 shows that D_e decreases from more than 26 kcal mol^{-1} for the C_s DI_1WI_1 structure of $BF_4^-(H_2O)_2$ to approximately 24 kcal mol^{-1} for the C_1 DI_1WI_1 minimum of $SiF_5^-(H_2O)_2$ and less than 23 kcal mol^{-1} for the C_s DI_1WI_1 structure of $PF_6^-(H_2O)_2$ at the CCSD(T)/haTZ level of theory.

The two water molecules do not interact with each other in the other four $SiF_5^-(H_2O)_2$ minima. Three of these water−anion dihydrates (C_2 DI_2, C_{2v} DI_2, and C_s $DI_2(A)$) have D_e values on par with that for the C_s DI_1WI_1 local minimum (around 23 kcal mol^{-1}) and exhibit similar hydrogen bond topologies in which each water molecule forms an asymmetric DIHB with the SiF_5^- ion with one short hydrogen bond to an axial F atom and a longer hydrogen bond to an equatorial F atom. In contrast, the remaining dihydrate minimum characterized for SiF_5^- has one water molecule that forms a symmetric DIHB with two equatorial F atoms, and the CCSD(T)/haTZ electronic energy of this C_s $DI_2(B)$ structure is nearly 3 kcal mol^{-1} higher than the C_1 DI_1WI_1 global minimum.

Despite the aforementioned trends in the dissociation energies (decreasing by several kcal mol^{-1} across the $BF_4^-(H_2O)_n$, $SiF_5^-(H_2O)_n$, $PF_6^-(H_2O)_n$ series), there is consistent and nearly perfect doubling of D_e from the monohydrate global minimum to the dihydrate global minimum for each anion. As n increases from 1 to 2 for $BF_4^-(H_2O)_n$, $SiF_5^-(H_2O)_n$, and $PF_6^-(H_2O)_n$, the corresponding CCSD(T)/haTZ D_e values increased by a factor of 2.01, 1.98, and 2.11, respectively. When the counterpoise (CP) procedure is applied to the SiF_5^- mono- and dihydrate global minima, the CCSD(T)/haTZ dissociation energies decrease by 6% or less to about 11.6 and 22.7 kcal mol^{-1}, respectively. These CP-corrected D_e values can be found in the Supporting Information.

3.1.2. $SiF_6^{2-}(H_2O)_n$. Similar to PF_6^-, the isolated SiF_6^{2-} ion has an octahedral structure with O_h symmetry with 6 symmetry-equivalent F atoms, and the monohydrate has a single minimum structure (C_{2v} DI_1) with a symmetric DIHB. This monohydrate minimum is shown in the top left image in Figure 2 with OH···F bond lengths of 1.84 Å at the CCSD(T)/haTZ level of theory. All of the monohydrate minima are structurally similar, but the 2− charge on silicon hexafluoride dramatically increases the dissociation energy. The CCSD(T)/haTZ D_e of $SiF_6^{2-}(H_2O)_1$ is 24.82 kcal mol^{-1} (top entry in last column of Table 1) which is approximately twice as large as the corresponding D_e values for the other three anions with a 1− charge.

Five minima have been identified for the $SiF_6^{2-}(H_2O)_2$ system starting from stationary points previously reported for $PF_6^-(H_2O)_2$.[22] The five SiF_6^{2-} dihydrates are pictured in Figure 2 alongside the C_{2v} DI_1 monohydrate minimum. These dihydrate structures are nearly structurally identical to those previously reported for PF_6^- (Figures 1 and 2 from ref 22), including the C_s DI_1WI_1 dihydrate global minimum which is the only minimum with water−water contacts for both PF_6^- and SiF_6^{2-}. Both PF_6^- and SiF_6^{2-} have D_{2h}, C_2, and C_s dihydrates with only water−anion contacts. However, this study also identified an additional minimum, the C_{2v} DI_2 dihydrate structure that is a transition state for PF_6^- (C_{2v} Edge−Edge in Figure 2 of ref 22). The D_e values for these dihydrates can be seen in the last column of data in Table 1. An interesting finding for the SiF_6^{2-} dihydrates is the energetic competition between the five structures compared to the PF_6^- dihydrates. For instance, for PF_6^-, the C_s DI_1WI_1 global minimum dihydrate is more than 2 kcal mol^{-1} lower in energy than the D_{2h} DI_2 structure (referred to as D_{2h} Edge−Edge in that study), but the analogous $SiF_6^{2-}(H_2O)_2$ structures are separated by less than 0.1 kcal mol^{-1} on the CCSD(T)/haTZ potential energy surface. In fact, there are three DI_2 local minima within *ca.* 0.2 kcal mol^{-1} of the $SiF_6^{2-}(H_2O)_2$ DI_1WI_1 global minimum, and a fourth lies only about 1 kcal mol^{-1} higher.

The CCSD(T)/haTZ dissociation energy of the $SiF_6^{2-}(H_2O)_2$ global minimum was found to be almost 48 kcal mol^{-1} and nearly double that of the monohydrate (larger by a factor of 1.91). When the CP procedure is applied to the SiF_6^{2-} global minimum mono- and dihydrate structures, the CCSD(T)/haTZ dissociation energies decrease by at most 4% to 23.9 and 45.9 kcal mol^{-1}, respectively. The D_e values computed with the CP procedure for these two minima can be found in the Supporting Information.

https://doi.org/10.1021/acs.jpca.4c03430
J. Phys. Chem. A 2024, 128, 5637−5645

3.2. Vibrational Frequencies. Table 2 displays the shifts in the harmonic OH stretching frequencies that are exhibited by the global minimum monohydrate structures observed when water binds to either the BF_4^- tetrahedron, SiF_5^- trigonal bipyramid, or either of the PF_6^- or SiF_6^{2-} octahedra. These values are relative to the OH stretching frequencies (ω) for an isolated water molecule, where the harmonic vibrational frequency of the symmetric a_1 mode is 3814 cm^{-1}, and that of the antisymmetric b_2 mode is 3924 cm^{-1} at the CCSD(T)/haTZ level of theory. These reference values are provided in the first two columns of data in Table 2. The irreducible representations associated with the OH stretching vibrations of each monohydrate do not always directly correspond to the a_1 and b_2 irreducible representations of the C_{2v} point group (such as the C_s DI_1 $SiF_5^-(H_2O)_1$ structure). In such cases, each mode can still be classified as predominantly pseudosymmetric or pseudoantisymmetric in order to determine the appropriate reference mode for calculating each frequency shift ($\Delta\omega$), and the same approach is used for the dihydrates (*vide infra*). While Table 2 shows the shifts for only the monohydrate global minima, in the case of SiF_5^- for which a second monohydrate local minimum was identified, the C_{2v} DI_1 shifts can be found in the Supporting Information.

The magnitude of the maximum frequency shift for each monohydrate grows steadily with D_e, and there is a pronounced increase when the charge doubles for silicon hexafluoride: $PF_6^-(H_2O)_1 < SiF_5^-(H_2O)_1 < BF_4^-(H_2O)_1 \ll SiF_6^{2-}(H_2O)_1$. The (pseudo)symmetric and (pseudo)-antisymmetric shifts are quite similar for $SiF_5^-(H_2O)_1$ (within 20 cm^{-1}), but they are quite different for the other monohydrates (separated by at least 55 cm^{-1} and as much as 130 cm^{-1}).

Table 3 lists the OH stretching frequency shifts for the SiF_5^- dihydrates. The four $\Delta\omega$ values for each structure are listed such that the top two values are in reference to the symmetric a_1 stretch of an isolated water molecule, and the bottom two values are in reference to the antisymmetric b_2 stretch of H_2O. The $\Delta\omega$ values for the structures in which both water molecules adopt an asymmetric DIHB motif between an axial F and equatorial F (C_2 DI_2, C_{2v} DI_2, and C_s DI_2(A)) fall into a fairly narrow distribution and are quite similar to those for the C_s DI_1 monohydrate in which water is bound in a similar manner. The pseudosymmetric OH stretching frequency for the C_s DI_1 structure shifts to lower energy by −88 cm^{-1} using CCSD(T)/haTZ, while the pseudoantisymmetric mode shifts to lower energy by −69 cm^{-1}, as shown in Table 2. Similarly, the pseudosymmetric OH stretches for the three dihydrates with only asymmetric, axially bound DIHBs shift to lower energy by −65 ± 19 cm^{-1} at the same level of theory. The corresponding shifts for the pseudoantisymmetric OH stretches fall into a more narrow range of $\Delta\omega$ values of −61 ± 5 cm^{-1}.

The SiF_5^- dihydrates which contain solvent−solvent interactions exhibit larger shifts in the OH stretching frequencies compared to the dihydrates with only solvent−solute contacts. The shifts in the OH stretching frequencies exceed −100 cm^{-1} for one mode in the C_s DI_1WI_1 local minimum and for three modes in the C_1 DI_1WI_1 global minimum (up to a maximum shift of −151 cm^{-1}).

Table 4 displays the shifts in the OH stretching frequencies induced by hydrogen bonding for the SiF_6^{2-} dihydrate minima along with those previously reported for the analogous $BF_4^-(H_2O)_2$ and $PF_6^-(H_2O)_2$ structures.[21,22] However, some of the CCSD(T)/haTZ frequency shifts for the latter system

Table 3. Shifts in the CCSD(T)/haTZ Harmonic OH Stretching Frequencies ($\Delta\omega$ in cm^{-1}) Induced by Hydrogen Bonding in the SiF_5^- Dihydrate Minima along with the Irreducible Representations (irrep) Associated with Each Vibrational Mode

irrep	$\Delta\omega$	irrep	$\Delta\omega$
C_1 DI_1WI_1		C_s DI_1WI_1	
a	−151	a′	−82
a	−101	a′	−57
a	−105	a′	−127
a	−78	a″	−95
C_2 DI_2		C_s DI_2(A)	
b	−72	a″	−55
a	−71	a′	−46
a	−64	a″	−66
b	−63	a′	−64
C_{2v} DI_2		C_s DI_2(B)	
b_2	−83	a′	−71
a_1	−81	a′	−31
b_2	−59	a″	−67
a_1	−56	a′	−65

Table 4. Shifts in the CCSD(T)/haTZ Harmonic OH Stretching Frequencies ($\Delta\omega$ in cm^{-1}) Induced by Hydrogen Bonding in the BF_4^-, PF_6^- and SiF_6^{2-} Dihydrate Minima along with the Irreducible Representations (irrep) Associated with Each Vibrational Mode

$BF_4^-(H_2O)_2$		$PF_6^-(H_2O)_2$		$SiF_6^{2-}(H_2O)_2$	
irrep	$\Delta\omega$[a]	irrep	$\Delta\omega$[b]	irrep	$\Delta\omega$
C_s DI_1WI_1		C_s DI_1WI_1[c]		C_s DI_1WI_1	
a′	−98	a′	*−93*	a′	−260
a′	−64	a′	*−35*	a′	−195
a′	−134	a′	*−100*	a′	−209
a″	−129	a″	*−93*	a″	−323
D_{2d} DI_2		D_{2h} DI_2[d]		D_{2h} DI_2	
b_2	−34	b_{3u}	−13	b_{3u}	−137
a_1	−32	a_g	−12	a_g	−134
e	−94	b_{1g}	−63	b_{1g}	−256
e	−94	b_{2u}	−62	b_{2u}	−251
C_s DI_2		C_2 DI_2[d]		C_2 DI_2	
a″	−36	b	−15	b	−134
a′	−35	a	−14	a	−131
a″	−89	a	−61	a	−254
a′	−85	b	−61	b	−252
		C_s DI_2[d]		C_{2v} DI_2	
		a″	*−15*	b_2	−170
		a′	*−14*	a_1	−167
		a″	*−61*	b_2	−213
		a′	*−58*	a_1	−202
				C_s DI_2	
				a″	−169
				a′	−162
				a″	−204
				a′	−193

[a]Ref 21. [b]Ref 22 with corrected values in italics. [c]Labeled as "WW-Edge-Face" structure in ref 22. [d]Labeled as "Edge−Edge" structure in ref 22.

https://doi.org/10.1021/acs.jpca.4c03430
J. Phys. Chem. A 2024, 128, 5637−5645

were incorrectly reported in Table 3 of ref 22, and the updated values are presented here as italicized entries in Table 4 (see C_s DI_1WI_1 and C_s DI_2). The $\Delta\omega$ values for each structure in Table 4 are listed in the same order as those in Table 3.

When comparing the $\Delta\omega$ values for the solvent−solute dihydrates of BF_4^-, SiF_5^-, and PF_6^-, the same general pattern is observed as what was shown for the monohydrates. That is, the maximum OH stretching frequency shifts for the structures exhibiting only solvent−solute contacts consistently grow larger as D_e increases. Specifically, these values are −63 cm^{-1} for $PF_6^-(H_2O)_2$, − 83 cm^{-1} for $SiF_5^-(H_2O)_2$, and −94 cm^{-1} for $BF_4^-(H_2O)_2$. The maximum magnitude of the shifts associated with the analogous $SiF_6^{2-}(H_2O)_2$ minima are much larger (exceeding 200 cm^{-1} for each DI_2 structure).

All of the dihydrates identified in this study with solvent−solvent contacts exhibit larger shifts in the OH stretching frequencies than their solvent−solute counterparts. The DI_1WI_1 isomers of the three singly charged anions each have maximum frequency shift values that are at least −100 cm^{-1}, with $PF_6^-(H_2O)_2$ having the smallest maximum shift at −100 cm^{-1} and $SiF_5^-(H_2O)_2$ having the largest at −151 cm^{-1}. However, the maximum shift observed for the C_s DI_1WI_1 $SiF_6^{2-}(H_2O)_2$ global minimum jumps to −323 cm^{-1}.

The solvent−solute interactions also induce vibrational frequency shifts in the SiF stretching modes of the SiF_5^- and SiF_6^{2-} anions, but they tend to be appreciably smaller than the observed OH stretching frequency shifts. (See Supporting Information.) Overall, this is consistent with the BF and PF shifts previously reported for the microhydration of BF_4^- and PF_6^-, respectively.[21,22] For SiF_5^-, the formation of the monohydrate structures induces SiF harmonic vibrational frequency shifts to lower energy for some modes and higher energy for others. The maximum SiF shifts observed for the $SiF_5^-(H_2O)_1$ system are for the C_{2v} DI_1 local minimum for which the largest increase is +21 cm^{-1} and the largest decrease is −31 cm^{-1}. Aside from the +19 cm^{-1} outlier observed for the C_s DI_1 global minimum, the remaining $SiF_5^-(H_2O)_1$ SiF shifts fall into a range of ±9 cm^{-1}. Compared with the BF and PF vibrational frequency shifts observed for $BF_4^-(H_2O)_1$ and $PF_6^-(H_2O)_1$, respectively, the trend continues in which BF_4^- exhibits the largest shifts while PF_6^- exhibits the smallest shifts ($PF_6^- < SiF_5^- < BF_4^-$). For $SiF_6^{2-}(H_2O)_1$, the maximum shift in the SiF stretching frequencies is −28 cm^{-1}, with the remaining frequencies shifting by ±9 cm^{-1}. The largest SiF frequency shifts observed for $SiF_5^-(H_2O)_2$ are for the C_{2v} DI_2 local minimum in which one mode shifts by +35 cm^{-1} to higher energy, and another shifts by −26 cm^{-1} to lower energy. Most of the other dihydrates exhibit similar shifts, with the lowest overall exhibited by the C_s DI_2(B) structure. In comparison, the SiF shifts observed for $SiF_6^{2-}(H_2O)_2$ are generally larger than those for $SiF_5^-(H_2O)_2$, which follows the trend observed for the dissociation energies and OH stretching frequency shifts. However, the magnitudes of the $SiF_6^{2-}(H_2O)_2$ SiF shifts are significantly smaller than the OH shifts. The C_{2v} DI_2 structure of the SiF_6^{2-} dihydrate exhibits the most pronounced shifts in the harmonic SiF stretching frequencies for which the largest increase is +26 cm^{-1} and the largest decrease is −39 cm^{-1}. The SiF frequency shifts for all SiF_5^- and SiF_6^{2-} mono- and dihydrate minima can be found in the Supporting Information.

4. CONCLUSIONS

Two monohydrate and six dihydrate configurations have been identified as minima at the CCSD(T)/haTZ level of theory for the $SiF_5^-(H_2O)_n$ systems through systematic distribution of up to two water molecules around the faces and edges of the anion's trigonal bipyramidal structure. One monohydrate and five dihydrate minima have also been identified for the $SiF_6^{2-}(H_2O)_n$ systems using previously reported $PF_6^-(H_2O)_n$ geometries as starting structures. None of these hydrated structures have been reported elsewhere to the best of our knowledge.

For the $SiF_5^-(H_2O)_1$ system, the identified C_{2v} DI_1 minimum features a typical, symmetric DIHB with the water molecule bridging two equatorial F atoms of the anion. Because of the anion's trigonal bipyramidal structure with slightly more negative charge accumulated on the axial F atoms,[46] another unique monohydrate minimum was identified in which water binds in an asymmetric DIHB motif with one axial and one equatorial F atom. Interestingly, this second minimum, C_s DI_1, has an electronic energy that is more than 2 kcal mol^{-1} lower than that of the C_{2v} DI_1 local minimum. The preference for this asymmetric DIHB motif extends to the dihydrates of SiF_5^-.

When comparing the hydrated structures of SiF_5^- with those previously reported for BF_4^- and PF_6^-, a trend is observed in which the dissociation energies exhibited by the mono- and dihydrate global minima increase as the singly charged anions get smaller. The largest of these three anions, PF_6^-, exhibits D_e values of approximately 10 kcal mol^{-1} for the monohydrate and 22 kcal mol^{-1} for the dihydrate global minimum with CCSD(T)/haTZ.[22] The dissociation energies for SiF_5^- are slightly larger, with the $SiF_5^-(H_2O)_1$ global minimum having a D_e of approximately 12 kcal mol^{-1} and the $SiF_5^-(H_2O)_2$ global minimum having a D_e of approximately 24 kcal mol^{-1}. The BF_4^- global minimum mono- and dihydrate structures have the largest D_e values at approximately 13 and 26 kcal mol^{-1}, respectively.[21] This trend carries through to the harmonic vibrational frequency shifts ($\Delta\omega$), where the largest shifts observed for the monohydrates and the dihydrates with only solvent−solute contacts increase as the singly charged anions get smaller ($PF_6^- < SiF_5^- < BF_4^-$). For both the dissociation energies and the $\Delta\omega$ values, however, there is a pronounced increase when the charge on the anion doubles as in the case of SiF_6^{2-}. The D_e for the $SiF_6^{2-}(H_2O)_1$ global minimum is approximately 24 kcal mol^{-1}, and the D_e for the $SiF_6^{2-}(H_2O)_2$ global minimum is approximately 47 kcal mol^{-1} at the CCSD(T)/haTZ level of theory. While the $\Delta\omega$ values for the singly charged anions do not exceed −129 cm^{-1} for the monohydrate global minima, the SiF_6^{2-} C_{2v} DI_1 structure exhibits a shift as large as −289 cm^{-1}. The shifts for the dihydrates with only solvent−solute contacts are also much larger for SiF_6^{2-} than for BF_4^-, SiF_5^-, and PF_6^-. While these shifts are no larger than −94 cm^{-1} for BF_4^-, − 83 cm^{-1} for SiF_5^-, and −63 cm^{-1} for PF_6^-, the smallest shift displayed by a solvent−solute $SiF_6^{2-}(H_2O)_2$ minimum is −131 cm^{-1}.

For all four anions, the dihydrates with solvent−solvent interactions exhibit larger shifts in the OH stretching frequencies compared to the dihydrates with only solvent−solute contacts. Structures with water−water contacts display shifts of at least −100 cm^{-1} for one or more modes for the singly charged anions, and $\Delta\omega$ grows as large as −323 cm^{-1} for the $SiF_6^{2-}(H_2O)_2$ global minimum at the CCSD(T)/haTZ

https://doi.org/10.1021/acs.jpca.4c03430
J. Phys. Chem. A 2024, 128, 5637−5645

level of theory. These findings further demonstrate the importance of solvent−solvent interactions in addition to solvent−solute contacts when characterizing the structures, energetics, and spectroscopic signatures of hydrated ions such as BF_4^-, SiF_5^-, PF_6^-, or SiF_6^{2-}.

■ ASSOCIATED CONTENT

Supporting Information

The Supporting Information is available free of charge at https://pubs.acs.org/doi/10.1021/acs.jpca.4c03430.

Cartesian coordinates, electronic dissociation energies computed with the CP procedure, and harmonic vibrational frequencies (PDF)

■ AUTHOR INFORMATION

Corresponding Author

Gregory S. Tschumper − *Department of Chemistry and Biochemistry, University of Mississippi, University, Mississippi 38677−1848, United States;* orcid.org/0000-0002-3933-2200; Phone: +1 662 915 7301; Email: tschumpr@olemiss.edu; Fax: +1 662 915 7300

Author

Jacquelyn J. Mosely − *Department of Chemistry and Biochemistry, University of Mississippi, University, Mississippi 38677−1848, United States*

Complete contact information is available at: https://pubs.acs.org/10.1021/acs.jpca.4c03430

Notes

The authors declare no competing financial interest.

■ ACKNOWLEDGMENTS

This work was supported in part by the National Science Foundation (CHE-2154403). The Mississippi Center for Supercomputing Research (MCSR) is also thanked for a generous allocation of time on their computational resources.

■ REFERENCES

(1) Collins, K. D. Ion hydration: Implications for cellular function, polyelectrolytes, and protein crystallization. *Biophys. Chem.* **2006**, *119*, 271−281.

(2) Yan, C.; Xue, Z.; Zhao, W.; Wang, J.; Mu, T. Surprising Hofmeister Effects on the Bending Vibration of Water. *ChemPhysChem* **2016**, *17*, 3309−3314.

(3) Zhang, Y.; Cremer, P. S. Interactions between macromolecules and ions: the Hofmeister series. *Curr. Opin. Chem. Biol.* **2006**, *10*, 658−663.

(4) Tobias, D. J.; Hemminger, J. C. Getting Specific About Specific Ion Effects. *Science* **2008**, *319*, 1197−1198.

(5) Gregory, K. P.; Elliott, G. R.; Robertson, H.; Kumar, A.; Wanless, E. J.; Webber, G. B.; Craig, V. S. J.; Andersson, G. G.; Page, A. J. Understanding specific ion effects and the Hofmeister series. *Phys. Chem. Chem. Phys.* **2022**, *24*, 12682−12718.

(6) Ao, H.; Chen, C.; Hou, Z.; Cai, W.; Liu, M.; Jin, Y.; Zhang, X.; Zhu, Y.; Qian, Y. Electrolyte solvation structure manipulation enables safe and stable aqueous sodium ion batteries. *J. Mater. Chem. A* **2020**, *8*, 14190−14197.

(7) Nian, Q.; Zhu, W.; Zheng, S.; Chen, S.; Xiong, B.-Q.; Wang, Z.; Wu, X.; Tao, Z.; Ren, X. An Overcrowded Water-Ion Solvation Structure for a Robust Anode Interphase in Aqueous Lithium-Ion Batteries. *ACS Appl. Mater. Interfaces* **2021**, *13*, 51048−51056.

(8) Shi, X.; Xie, J.; Wang, J.; Xie, S.; Yang, Z.; Lu, X. A weakly solvating electrolyte towards practical rechargeable aqueous zinc-ion batteries. *Nat. Commun.* **2024**, *15*, 302.

(9) Seddon, K. R.; Stark, A.; Torres, M.-J. Influence of chloride, water, and organic solvents on the physical properties of ionic liquids. *Pure Appl. Chem.* **2000**, *72*, 2275−2287.

(10) Blanchard, L. A.; Gu, Z.; Brennecke, J. F. High-Pressure Phase Behavior of Ionic Liquid/CO_2 Systems. *J. Phys. Chem. B* **2001**, *105*, 2437−2444.

(11) Sharma, A.; Ghorai, P. K. Effect of water on structure and dynamics of [BMIM][PF_6] ionic liquid: An all-atom molecular dynamics simulation investigation. *J. Chem. Phys.* **2016**, *144*, 114505.

(12) Combariza, J. E.; Kestner, N. R.; Jortner, J. Energy-structure relationships for microscopic solvation of anions in water clusters. *J. Chem. Phys.* **1994**, *100*, 2851−2864.

(13) Schneider, H.; Vogelhuber, K. M.; Weber, J. M. Infared spectroscopy of anionic hydrated fluorobenzenes. *J. Chem. Phys.* **2007**, *127*, 114311.

(14) Robertson, W. H.; Price, E. A.; Weber, J. M.; Shin, J.-W.; Weddle, G. H.; Johnson, M. A. Infrared Signatures of a Water Molecule Attached to Triatomic Domains of Molecular Anions: Evolution of the H-bonding Configuration with Domain Length. *J. Phys. Chem. A* **2003**, *107*, 6527−6532.

(15) Robertson, W. H.; Johnson, M. A. Molecular Aspects of Halide Ion Hydration: The Cluster Approach. *Annu. Rev. Phys. Chem.* **2003**, *54*, 173−213.

(16) Myshakin, E. M.; Jordan, K. D.; Robertson, W. H.; Weddle, G. H.; Johnson, M. A. Dominant structural motifs of $NO^-\cdot(H_2O)_n$ complexes: Infrared spectroscopic and ab initio studies. *J. Chem. Phys.* **2003**, *118*, 4945−4953.

(17) Robertson, W. H.; Johnson, M. A.; Myshakin, E. M.; Jordan, K. D. Isolating the Charge-Transfer Component of the Anionic H Bond Via Spin Suppression of the Intracluster Proton Transfer Reaction in the $NO^-\cdot H_2O$ Entrance Channel Complex. *J. Phys. Chem. A* **2002**, *106*, 10010−10014.

(18) Woronowicz, E. A.; Robertson, W. H.; Weddle, G. H.; Johnson, M. A.; Myshakin, E. M.; Jordan, K. D. Infrared Spectroscopic Characterization of the Symmetrical Hydration Motif in the $SO_2^-\cdot H_2O$ Complex. *J. Phys. Chem. A* **2002**, *106*, 7086−7089.

(19) Del Bene, J. E.; Alkorta, I.; Elguero, J. Microsolvation of the Be-F bond in complexes of BeF_2, BeF_3^{-1}, and BeF_4^{-2} with nH_2O, for n = 1 − 6. *Mol. Phys.* **2021**, *119*, e1933637.

(20) Wang, Y.; Li, H.; Han, S. A Theoretical Investigation of the Interactions between Water Molecules and Ionic Liquids. *J. Phys. Chem. B* **2006**, *110*, 24646−24651.

(21) Olive, L. N.; Dornshuld, E. V.; Schaefer, H. F., III; Tschumper, G. S. Competition between Solvent···Solvent and Solvent···Solute Interactions in the Microhydration of the Tetrafluoroborate Anion, $BF_4^-(H_2O)_{n=1,2,3,4}$. *J. Phys. Chem. A* **2023**, *127*, 8806−8820.

(22) Abdo, Y. A.; Tschumper, G. S. Competition between Solvent-Solvent and Solvent-Solute Interactions in the Microhydration of the Hexafluorophosphate Anion, $PF_6^-(H_2O)_{n=1,2}$. *J. Phys. Chem. A* **2020**, *124*, 8744−8752.

(23) Gutsev, G. L.; Boldyrev, A. I. DVM-Xα Calculations on the Ionization Potentials of MX_{k+1}^- Complex Anions and the Electron Affinities of MX_{k+1} "Superhalogens. *Chem. Phys.* **1981**, *56*, 277−283.

(24) Gutsev, G. L.; Boldyrev, A. I. The Electronic Structure of Superhalogens and Superalkalies. Russ. *Chem. Rev.* **1987**, *56*, 519−531.

(25) Seymour, J. M.; Gousseva, E.; Large, A. I.; Clarke, C. J.; Licence, P.; Fogarty, R. M.; Duncan, D. A.; Ferrer, P.; Venturini, F.; Bennett, R. A.; et al. Experimental measurement and prediction of ionic liquid ionisation energies. *Phys. Chem. Chem. Phys.* **2021**, *23*, 20957−20973.

(26) Srivastava, A. K.; Kumar, A.; Misra, N. Superhalogens as Building Blocks of Ionic Liquids. *J. Phys. Chem. A* **2021**, *125*, 2146−2153.

(27) Srivastava, A. K. Recent progress on the design and applications of superhalogens. *Chem. Commun.* **2023**, *59*, 5943−5960.

(28) Li, Y.; Wu, D.; Li, Z.-R. Compounds of Superatom Clusters: Preferred Structures and Significant Nonlinear Optical Properties of the BLi_6-X (X = F, LiF_2, BeF_3, BF_4) Motifs. *Inorg. Chem.* **2008**, *47*, 9773−9778.
(29) Giri, S.; Behera, S.; Jena, P. Superalkalis and Superhalogens As Building Blocks of Supersalts. *J. Phys. Chem. A* **2014**, *118*, 638−645.
(30) Xu, L.-N.; Li, Y.; Liu, J.-Y.; Wu, D.; Sun, Y.-B.; Li, Z.-R. Comparative study of hydrogenated and lithiated superhalogens. *Chem. Phys. Lett.* **2016**, *661*, 94−99.
(31) Srivastava, A. K.; Misra, N. Superbases and superacids form supersalts. *Chem. Phys. Lett.* **2016**, *644*, 1−4.
(32) Reddy, G. N.; Kumar, A. V.; Parida, R.; Chakraborty, A.; Giri, S. Zintl superalkalis as building blocks of supersalts. *J. Mol. Model.* **2018**, *24*, 306.
(33) King, R. A.; Mastryukov, V. S.; Schaefer, H. F., III The electron affinities of the silicon fluorides SiF_n (n = 1−5. *J. Chem. Phys.* **1996**, *105*, 6880−6886.
(34) Marchaj, M.; Freza, S.; Skurski, P. Why are SiX_5^- and GeX_5^- Stable but Not CF_5^- and CCl_5^-? *J. Phys. Chem. A* **2012**, *116*, 1966−1973.
(35) Sikorska, C.; Smuczyńska, S.; Skurski, P.; Anusiewicz, I. BX_4^- and AlX_4^- Superhalogen Anions (X = F, Cl, Br): An ab Initio Study. *Inorg. Chem.* **2008**, *47*, 7348−7354.
(36) Danten, Y.; Cabaço, M. I.; Besnard, M. Interaction of Water Highly Diluted in 1-Alkyl-3-methyl Imidazolium Ionic Liquids with the PF_6^- and BF_4^- Anions. *J. Phys. Chem. A* **2009**, *113*, 2873−2889.
(37) Son, H.; Nam, D.; Park, S. Real-Time Probing of Hydrogen-Bond Exchange Dynamics in Aqueous $NaPF_6$ Solutions by Two-Dimensional Infrared Spectroscopy. *J. Phys. Chem. B* **2013**, *117*, 13604−13613.
(38) Sikorska, C. Toward predicting vertical detachment energies for superhalogen anions exclusively from 2-D structures. *Chem. Phys. Lett.* **2015**, *625*, 157−163.
(39) Zaitsau, D. H.; Yermalayeu, A. V.; Emel'yanenko, V. N.; Butler, S.; Schubert, T.; Verevkin, S. P. Thermodynamics of Imidazolium-Based Ionic Liquids Containing PF_6 Anions. *J. Phys. Chem. B* **2016**, *120*, 7949−7957.
(40) Śmiechowski, M. Unusual Influence of Fluorinated Anions on the Stretching Vibrations of Liquid Water. *J. Phys. Chem. B* **2018**, *122*, 3141−3152.
(41) Srivastava, A. K.; Kumar, A.; Tiwari, S. N.; Misra, N. Application of superhalogens in the design of organic superconductors. *New J. Chem.* **2017**, *41*, 14847−14850.
(42) Qu, M.; Li, S.; Chen, J.; Xiao, Y.; Xiao, J. Ion transport in ionic liquid/poly(vinylidene fluoride) system under electric fields: A molecular dynamics simulation. *Colloids Surf. A: Physicochem. Eng. Asp.* **2022**, *642*, 128328.
(43) Jiao, Z.; Zhang, M.; Yang, L.; Wang, Y.; Fu, J. Liquid-Liquid Equilibrium for the Ternary System Water + 1-Methylimidazole + Ionic Liquid ([Hmim][PF_6], [Omim][PF_6], or [Omim][BF_4]) at 303.15 K. *J. Chem. Eng. Data* **2022**, *67*, 1474−1480.
(44) Sobczyk, M.; Sawicka, A.; Skurski, P. Theoretical Search for Anions Possessing Large Electron Binding Energies. *Eur. J. Inorg. Chem.* **2003**, *2003*, 3790−3797.
(45) Gutsev, G. L. Theoretical investigation on the existence of the SiF_6^- anion. *Chem. Phys. Lett.* **1991**, *184*, 305−309.
(46) Koval, V. V.; Minyaev, R. M.; Minkin, V. I. Geometric and electronic structures of silicon fluorides $SiF_n^{(n-4)-}$ (N = 4−6) and potential energy surfaces for dissociation reactions $SiF_5^- \rightarrow SiF_4 + F^-$ and $SiF_6^{2-} \rightarrow SiF_5^- + F^-$. *Int. J. Quantum Chem.* **2016**, *116*, 1358−1361.
(47) Degtyarenko, A. S.; Rusanov, E. B.; Bauzá, A.; Frontera, A.; Krautscheid, H.; Chernega, A. N.; Mokhir, A. A.; Domasevitch, K. V. Self-assembly cavitand precisely recognizing hexafluorosilicate: a concerted action of two coordination and twelve CH···F bonds. *Chem. Commun.* **2013**, *49*, 9018−9020.
(48) Tian, X.-Y.; Zhou, H.-L.; Fang, X.; Mo, Z.-W.; Xu, Y.-T.; Zhou, D.-D.; Zhang, J.-P. Diverse coordination polymers from a new bent dipyridyl-type ligand 3,6-di(pyridin-4-yl)-9H-carbazole. *CrystEngComm* **2017**, *19*, 6164−6169.
(49) Gopalakrishnan, M.; Krittametaporn, N.; Yoshinari, N.; Konno, T.; Sangtrirutnugul, P. Anion-templated assembly of multinuclear copper(II)-triazole complexes. *New J. Chem.* **2020**, *44*, 13764−13770.
(50) Śmiechowski, M.; Gojło, E.; Stangret, J. Ionic Hydration in $LiPF_6$, $NaPF_6$, and KPF_6 Aqueous Solutions Derived from Infrared HDO Spectra. *J. Phys. Chem. B* **2004**, *108*, 15938−15943.
(51) Wei, Q.; Zhang, M.; Zhou, D.; Li, X.; Bian, H.; Fang, Y. Ultrafast Hydrogen Bond Exchanging between Water and Anions in Concentrated Ionic Liquid Aqueous Solutions. *J. Phys. Chem. B* **2019**, *123*, 4766−4775.
(52) Ayala, R.; Martínez, J.; Pappalardo, R. R.; Sánchez Marcos, E. Theoretical Study of the Microsolvation of the Bromide Anion in Water, Methanol, and Acetonitrile: Ion-Solvent vs Solvent-Solvent Interactions. *J. Phys. Chem. A* **2000**, *104*, 2799−2807.
(53) Pathak, A. K.; Mukherjee, T.; Maity, D. K. Microhydration of NO_3^-: A Theoretical Study on Structure, Stability and IR Spectra. *J. Phys. Chem. A* **2008**, *112*, 3399−3408.
(54) Pathak, A. K.; Mukherjee, T.; Maity, D. K. Microhydration of X_2 Gas (X = Cl, Br, and I): A Theoretical Study on $X_2 \cdot nH_2O$ Clusters (n = 1−8). *J. Phys. Chem. A* **2008**, *112*, 744−751.
(55) Wen, H.; Huang, T.; Liu, Y.-R.; Jiang, S.; Peng, X.-Q.; Miao, S.-K.; Wang, C.-Y.; Hong, Y.; Huang, W. Structure, temperature effect and bonding order analysis of hydrated bromide clusters. *Chem. Phys.* **2016**, *479*, 129−142.
(56) Neogi, S. G.; Chaudhury, P. Structure and Spectroscopic Aspects of Water-Halide Ion Clusters: A Study Based on a Conjunction of Stochastic and Quantum Chemical Methods. *J. Comput. Chem.* **2013**, *34*, 471−491.
(57) Pathak, A. K. Theoretical study on microhydration of NO_3^- ion: Structure and polarizability. *Chem. Phys.* **2011**, *384*, 52−56.
(58) Likholyot, A.; Hovey, J. K.; Seward, T. M. Experimental and theoretical study of hydration of halide ions. *Geochim. Cosmochim. Acta* **2005**, *69*, 2949−2958.
(59) Ayala, R.; Martínez, J.; Pappalardo, R. R.; Sánchez Marcos, E. On the halide hydration study: Development of first-principles halide ion-water interaction potential based on a polarizable model. *J. Chem. Phys.* **2003**, *119*, 9538−9548.
(60) Bajaj, P.; Riera, M.; Lin, J. K.; Mendoza Montijo, Y. E.; Gazca, J.; Paesani, F. Halide Ion Microhydration: Structure, Energetics, and Spectroscopy of Small Halide-Water Clusters. *J. Phys. Chem. A* **2019**, *123*, 2843−2852.
(61) Møller, C.; Plesset, M. S. Note on an approximation treatment for many-electron systems. *Phys. Rev.* **1934**, *46*, 618−622.
(62) Bartlett, R. J. Many-Body Perturbation Theory and Coupled Cluster Theory for Electron Correlation in Molecules. *Annu. Rev. Phys. Chem.* **1981**, *32*, 359−401.
(63) Purvis, G. D.; Bartlett, R. J. A full coupled-cluster singles and doubles model: The inclusion of disconnected triples. *J. Chem. Phys.* **1982**, *76*, 1910.
(64) Raghavachari, K.; Trucks, G. W.; Pople, J. A.; Head-Gordon, M. A fifth-order perturbation comparison of electron correlation. *Chem. Phys. Lett.* **1989**, *157*, 479−483.
(65) Dunning, T. H., Jr. Gaussian Basis Sets for Use in Correlated Molecular Calculations. I. the Atoms Boron Through Neon and Hydrogen. *J. Chem. Phys.* **1989**, *90*, 1007−1023.
(66) Kendall, R. A.; Dunning, T. H., Jr.; Harrison, R. J. Electron Affinities of the First-Row Atoms Revisited. Systematic Basis Sets and Wave Functions. *J. Chem. Phys.* **1992**, *96*, 6796−6806.
(67) Woon, D. E.; Dunning, T. H., Jr. Gaussian basis sets for use in correlated molecular calculations. III. The atoms aluminum through argon. *J. Chem. Phys.* **1993**, *98*, 1358−1371.
(68) Kestner, N. R. He-He Interaction in the SCF-MO Approximation. *J. Chem. Phys.* **1968**, *48*, 252−257.
(69) Liu, B.; McLean, A. D. Accurate calculation of the attractive interaction of two ground state helium atoms. *J. Chem. Phys.* **1973**, *59*, 4557−4558.

https://doi.org/10.1021/acs.jpca.4c03430
J. Phys. Chem. A 2024, 128, 5637−5645

(70) Jansen, H.; Ros, P. Non-empirical molecular orbital calculations on the protonation of carbon monoxide. *Chem. Phys. Lett.* **1969**, *3*, 140−143.
(71) Boys, S.; Bernardi, F. The calculation of small molecular interactions by the differences of separate total energies. Some procedures with reduced errors. *Mol. Phys.* **1970**, *19*, 553−566.
(72) Simon, S.; Duran, M.; Dannenberg, J. J. How does basis set superposition error change the potential surfaces for hydrogen-bonded dimers? *J. Chem. Phys.* **1996**, *105*, 11024−11031.
(73) Tschumper, G. S. Reliable Electronic Structure Computations for Weak Non-Covalent Interactions in Clusters. *Rev. Comput. Chem.* **2008**, *26*, 39−90.
(74) Frisch, M. J.; Trucks, G. W.; Schlegel, H. B.; Scuseria, G. E.; Robb, M. A.; Cheeseman, J. R.; Scalmani, G.; Barone, V.; Petersson, G. A.; Nakatsuji, H.; Li, X.; Caricato, M.; Marenich, A. V.; Bloino, J.; Janesko, B. G.; Gomperts, R.; Mennucci, B.; Hratchian, H. P.; Ortiz, J. V.; Izmaylov, A. F.; Sonnenberg, J. L.; Williams-Young, D.; Ding, F.; Lipparini, F.; Egidi, F.; Goings, J.; Peng, B.; Petrone, A.; Henderson, T.; Ranasinghe, D.; Zakrzewski, V. G.; Gao, J.; Rega, N.; Zheng, G.; Liang, W.; Hada, M.; Ehara, M.; Toyota, K.; Fukuda, R.; Hasegawa, J.; Ishida, M.; Nakajima, T.; Honda, Y.; Kitao, O.; Nakai, H.; Vreven, T.; Throssell, K.; Montgomery, J. A., Jr.; Peralta, J. E.; Ogliaro, F.; Bearpark, M.; Heyd, J. J.; Brothers, E. N.; Kudin, K. N.; Staroverov, V. N.; Kobayashi, R.; Normand, J.; Raghavachari, K.; Rendell, A.; Burant, J. C.; Iyengar, S. S.; Tomasi, J.; Cossi, M.; Millam, J. M.; Klene, M.; Adamo, C.; Cammi, R.; Ochterski, J. W.; Martin, R. L.; Morokuma, K.; Farkas, O.; Foresman, J. B.; Fox, D. J. *Gaussian 16*, revision C.01; Gaussian, Inc.: Wallingford, CT, 2016.
(75) Frisch, M. J.; Trucks, G. W.; Schlegel, H. B.; Scuseria, G. E.; Robb, M. A.; Cheeseman, J. R.; Scalmani, G.; Barone, V.; Mennucci, B.; Petersson, G. A.; Nakatsuji, H.; Caricato, M.; Li, X.; Hratchian, H. P.; Izmaylov, A. F.; Bloino, J.; Zheng, G.; Sonnenberg, J. L.; Hada, M.; Ehara, M.; Toyota, K.; Fukuda, R.; Hasegawa, J.; Ishida, M.; Nakajima, T.; Honda, Y.; Kitao, O.; Nakai, H.; Vreven, T.; Montgomery, J. A., Jr.; Peralta, J. E.; Ogliaro, F.; Bearpark, M.; Heyd, J. J.; Brothers, E.; Kudin, K. N.; Staroverov, V. N.; Kobayashi, R.; Normand, J.; Raghavachari, K.; Rendell, A.; Burant, J. C.; Iyengar, S. S.; Tomasi, J.; Cossi, M.; Rega, N.; Millam, J. M.; Klene, M.; Knox, J. E.; Cross, J. B.; Bakken, V.; Adamo, C.; Jaramillo, J.; Gomperts, R.; Stratmann, R. E.; Yazyev, O.; Austin, A. J.; Cammi, R.; Pomelli, C.; Ochterski, J. W.; Martin, R. L.; Morokuma, K.; Zakrzewski, V. G.; Voth, G. A.; Salvador, P.; Dannenberg, J. J.; Dapprich, S.; Daniels, A. D.; Farkas, O.; Foresman, J. B.; Ortiz, J. V.; Cioslowski, J.; Fox, D. J. *Gaussian 09*, revision E.01; Gaussian, Inc.: Wallingford, CT, 2009.
(76) Matthews, D.; Cheng, L.; Harding, M.; Lipparini, F.; Stopkowicz, S.; Jagau, T.-C.; Szalay, P.; Gauss, J.; Stanton, J. Coupled-cluster techniques for computational chemistry: The CFOUR program package. *J. Chem. Phys.* **2020**, *152*, 214108.
(77) Werner, H. J.; Knowles, P. J.; Knizia, G.; Manby, F. R.; Schütz, M. Molpro: a general-purpose quantum chemistry program package. *WIREs Comput. Mol. Sci.* **2012**, *2*, 242−253.
(78) Werner, H. J.; Knowles, P. J.; Manby, F. R.; Black, J. A.; Doll, K.; Hesselmann, A.; Kats, D.; Köhn, A.; Korona, T.; Kreplin, D. A.; et al. The Molpro quantum chemistry package. *J. Chem. Phys.* **2020**, *152*, 144107.
(79) Werner, H.-J.; Knowles, P. J.; Celani, P.; Györffy, W.; Hesselmann, A.; Kats, D.; Knizia, G.; Köhn, A.; Korona, T.; Kreplin, D. et al. *MOLPRO, a package of ab initio programs*, version 1, 2022.
(80) Tschumper, G. S.; Leininger, M. L.; Hoffman, B. C.; Valeev, E. F.; Schaefer, H. F., III; Quack, M. Anchoring the water dimer potential energy surface with explicitly correlated computations and focal point analyses. *J. Chem. Phys.* **2002**, *116*, 690.
(81) Howard, J. C.; Gray, J. L.; Hardwick, A. J.; Nguyen, L. T.; Tschumper, G. S. Getting down to the Fundamentals of Hydrogen Bonding: Anharmonic Vibrational Frequencies of $(HF)_2$ and $(H_2O)_2$ from Ab Initio Electronic Structure Computations. *J. Chem. Theory Comput.* **2014**, *10*, 5426−5435.

https://doi.org/10.1021/acs.jpca.4c03430
J. Phys. Chem. A 2024, 128, 5637−5645